

## CLASSIFICATION OF BUILDING AREA USING SLANT ANGLE AND DENSITY INDICES DERIVED FROM POLARIMETRIC SAR DATA

S. Iwasa <sup>a,\*</sup>, J. Susaki <sup>b</sup>, M. Tamura <sup>b</sup>

<sup>a</sup> Department of Urban and Environmental Engineering, Graduate School of Engineering, Kyoto University, Kyotodaigaku-Katsura, Nishikyo-ku, Kyoto, 615-8540 Japan – miwasan1023@yahoo.co.jp

<sup>b</sup> Graduate School of Global Environmental Studies, Kyoto University, Kyotodaigaku-Katsura, Nishikyo-ku, Kyoto, 615-8540 Japan - junichi.susaki@at2.ecs.kyoto-u.ac.jp

Commission VIII, WG VIII/1

**KEY WORDS:** Urban extraction, POLSAR, POA (Polarization Orientation Angle), Entropy

### ABSTRACT:

Urban extraction is one of the most expected applications using remote sensing, but the automatic extraction has been challenging. Especially in the field of SAR applications, the complex scattering in the urban area is sensitive to the building spatial arrangement, and it prevents from the automatic extraction. Spaceborne Polarimetric synthetic aperture radar (POLSAR), an advanced approach to synthetic aperture radar (SAR), has been operated since PALSAR (Phased Array type L-band Synthetic Aperture Radar) onboard ALOS (Advanced Land Observing Satellite) was launched in 2006. Several indicators derived from POLSAR data have been developed to classify landcovers, and some of them have been utilized to extract the geometric features of the target. One of such indicators is Polarization Orientation Angle (POA), which is reported to estimate slant angle of the target. In addition, the indicators related to the density of the target are also proposed. Therefore, in this research, we examined the effectiveness of such polarimetric indices as urban structural detectors through a laboratory experiment, and we developed a classifier composed of the indices, which can be applicable for the satellite data. First, we measured the backscattering from the concrete blocks arranged in different slant angles and distances in an anechoic radio wave chamber. In this experiment, it was found the interrelation between spatial arrangement and such indicators as POA and density-related indicators. As a result, it is demonstrated that POA is a good detector for slant angle of man-made structures, and of all the indicators, entropy has the highest correlation with building density. Then, using satellite polarimetric data, we discriminated urban areas according to the classifier using POA and entropy. The comparison with aerial photo indicated that POA is an effective indicator to extract the slant buildings and that there are some areas where entropy distinguishes the difference of building density.

### 1. INTRODUCTION

From the viewpoint of city planning or disaster prevention, spatial arrangement and structures of buildings in urban areas are important data. While accurate measurement of such urban features using terrestrial sensors such as LiDAR (Light Detection and Ranging) is quite costly, the airborne or spaceborne sensors are expected to measure the wide-spread data at a relatively low-cost. Especially synthetic aperture radar (SAR) is highly expected for immediate observation after disasters and so on, for it is available even at night or in bad weather. However, accurate urban monitoring by SAR has been difficult so far, because the result is seriously affected by relative slant angle of measured buildings to observation direction.

Polarimetric synthetic aperture radar (POLSAR), an advanced approach to SAR is reported to detect various information of land surface which cannot be acquired by optical sensor. Several indicators derived from POLSAR data have been developed, and some of them have been utilized to extract the geometric features of the target. One of such indicators is Polarization Orientation Angle (POA), which is reported to estimate slant angle of the target (Kimura *et al.*, 2005). In

addition, the indicators related to the density of the target are also proposed. Utilizing these indices in urban area, reliability of monitoring could be better.

Therefore, the objective of this research is to improve the accuracy of extraction of urban area from POLSAR data, and we aim at the method which is independent of slant angle and can detect spatial arrangement (density, height) of the buildings.

### 2. USED INDICES

POLSAR data has the complex scattering matrix given by

$$S = \begin{pmatrix} S_{hh} & S_{hv} \\ S_{vh} & S_{vv} \end{pmatrix} = \begin{pmatrix} a & c \\ c & b \end{pmatrix} \quad (1)$$

assuming that  $S_{hv}$  and  $S_{vh}$  are equivalent. The indices shown in this section are derived from this scattering matrix. Further, some indices utilize the coherency matrix represented by

$$T = \begin{pmatrix} T_{11} & T_{12} & T_{13} \\ T_{21} & T_{22} & T_{23} \\ T_{31} & T_{32} & T_{33} \end{pmatrix} \quad (2)$$

$$= \begin{pmatrix} |a+b|^2 & (a+b)(a-b)^* & 2(a+b)c^* \\ (a-b)(a+b)^* & |a-b|^2 & 2(a-b)c^* \\ 2c(a+b)^* & 2c(a-b)^* & 4|c|^2 \end{pmatrix}$$

### 2.1 Polarization Orientation Angle (POA)

Polarization Orientation Angle  $\theta$  compensates scattering matrix as follows

$$S(\theta) = \begin{pmatrix} \cos \theta & \sin \theta \\ -\sin \theta & \cos \theta \end{pmatrix} \begin{pmatrix} a & c \\ c & b \end{pmatrix} \begin{pmatrix} \cos \theta & -\sin \theta \\ \sin \theta & \cos \theta \end{pmatrix} \quad (3)$$

$\theta$  is determined so that the target would stand perpendicular to the orbit

$$\theta = \frac{1}{4} \tan^{-1} \left( \frac{4 \operatorname{Re}(|a-b|c^*)}{|a-b|^2 - 4|c^*|^2} \right) \quad \left( -\frac{\pi}{4} \leq \theta \leq \frac{\pi}{4} \right) \quad (4)$$

This is the same as the minimization of  $T_{33}$  element of coherency matrix, and POA is equal to the phase term of circular polarization coefficient. POA is reported to estimate slant angle of the target.

### 2.2 Entropy (Cloude and Pottier, 1997)

Coherency matrix can be diagonalized using unitary matrix  $U$  as follows

$$T = \begin{pmatrix} T_{11} & T_{12} & T_{13} \\ T_{21} & T_{22} & T_{23} \\ T_{31} & T_{32} & T_{33} \end{pmatrix} = U \begin{pmatrix} \lambda_1 & 0 & 0 \\ 0 & \lambda_2 & 0 \\ 0 & 0 & \lambda_3 \end{pmatrix} U^* \quad (5)$$

where  $\lambda_1$ ,  $\lambda_2$  and  $\lambda_3$  are the eigenvalue of the matrix  $T$ . Entropy  $H$  is given by

$$H = -\sum_{i=1}^3 P_i \log_3 P_i \quad (6)$$

where

$$P_i = \frac{\lambda_i}{\lambda_1 + \lambda_2 + \lambda_3} \quad (i=1,2,3) \quad (7)$$

Entropy shows the randomness of scattering. Only surface scattering would occur in  $H=0$ , while various scattering (e.g. surface scattering, volume scattering, double bounce scattering) would randomly occur in  $H=1$ . Entropy is often used in land cover classification.

### 2.3 Four-Component Decomposition (Yamaguchi *et al.*, 2005)

Four-component decomposition has been developed from three-component decomposition (Freeman and Durban, 1998). In this method, measured polarimetric scattering wave is decomposed into scattering components based on physical scattering process: surface scattering (Ps), volume scattering (Pv), double bounce scattering (Pd), and helix scattering (Pc). Scattering matrix is decomposed into the summation of the basic scattering matrices of the four components, and then coefficients of the four matrices are calculated, which determines the power of each component.

### 2.4 Target Decomposition Method (Dong *et al.*, 1998)

Dong *et al.* proposed another decomposition model that is fit for urban structures. The components derived after decomposition are double bounce scattering (DB), odd bounce scattering (OB), bragg scattering (BS), and cross-polarized scattering (CS).

## 3. ANALYSIS OF X-BAND EXPERIMENTAL DATA

### 3.1 Experiment

On September 8 and 29, 2009, we carried out an experiment in the anechoic radio wave chamber in Wave Engineering laboratory, Department of Information Engineering, Faculty of Engineering, Niigata University. One of the purposes is to examine whether POA is sensitive to slant angle of man-made targets, the other is to judge which index has the strong correlation with density of them. Used radar system and object are explained below.

**3.1.1 Radar System:** The polarimetric measurement system which is capable of synthetic aperture process was used. Figure 1 shows the radar and the zoom of its antennas. The wave frequency is X-band (10 GHz), the antenna height is 180 cm, and the incident angle is 45°.

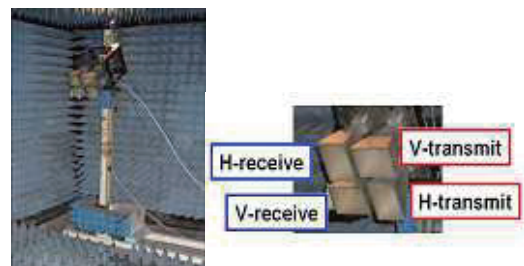


Figure 1. (Left) Radar system for the experiment. (Right) Zoom of its antennas. Each of the four antennas corresponds to horizontal polarization transmit, horizontal polarization receive, vertical polarization transmit, and vertical polarization receive.

**3.1.2 Object to Measure:** Nine concrete block cubes were arranged to measure and analyze the backscattering. The cube has 10-cm length, and the arrangement of the blocks is displayed in Figure 2. As illustrated in the figure, blocks were placed on 3×3 grid. The slant angle of the structure was defined as 0° when the side of the blocks are perpendicular to the radar path. First, the structure was measured at 0°, then the whole structure was rotated right-handedly in steps of 15°. Following the same procedure, the data at six slant angles were measured. Moreover, at each slant angle, the structure was measured three times with the distance of blocks 10 cm, 15 cm, and 20 cm, i.e., the measurement was done eighteen times in total.

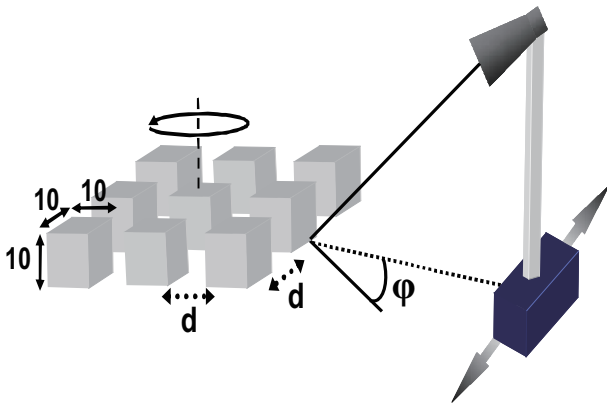


Figure 2. Schematic diagram of the measured structure.  $d$  is the distance of the blocks (three distances),  $\phi$  is the slant angle of the blocks (six angles).

**3.2 Results and Discussion**

From the data acquired in the experiment, each index described in the previous section was calculated.

Figure 3 shows the relationship between POA and the slant angle of the blocks. It was found that POA and actual slant angle have linear relationship when slant angle is set between 15° and 75°. Moreover, in the analysis using four-component decomposition (Iwasa *et al.*, 2009), it is proved that  $P_s$  and  $P_d$  become greater if buildings are perpendicular to the radar path (the result is shown in Figure 4); thus slant angle of the building may be estimated using four-components together with POA.

Next, Figure 5 demonstrates the relationship between entropy and the distance of the blocks. Entropy increases in all slant angles when the distance changes from 10 cm to 15 cm, while it decreases in almost all the slant angles when the distance changes from 15 cm to 20 cm. Therefore, entropy and building density may have nonlinear relationship. Furthermore, the relationship between four-components and the distance of the blocks is shown in Figure 6. As seen in figures, no component has better correlation with the distance than entropy. Target Decomposition Method was also investigated, and it was found

that it did not show good relationship with the distance of the blocks, either.

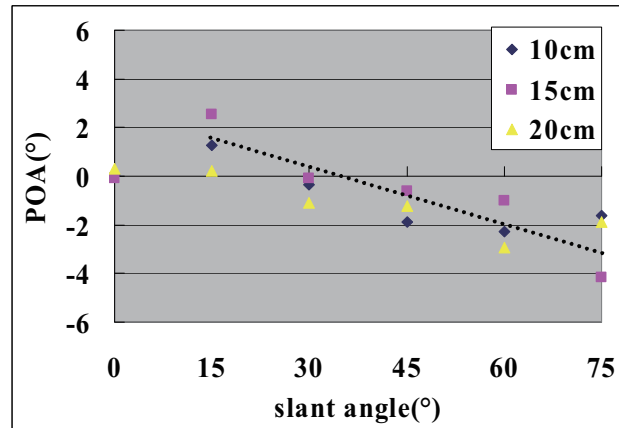


Figure 3. Relationship between POA and the slant angle of the blocks.

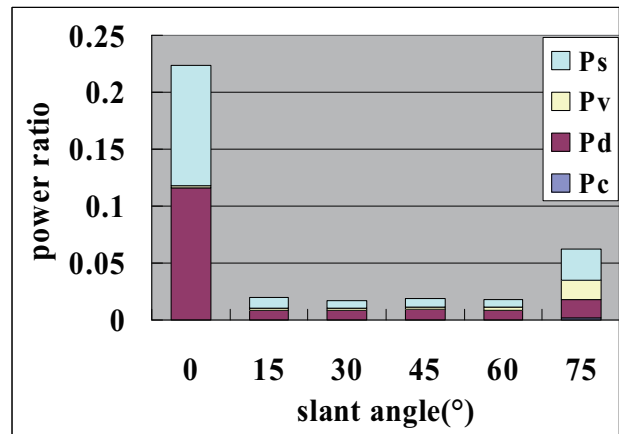


Figure 4. Relationship between four-components and the slant angle of the blocks. Power ratio in the vertical axis means the ratio to the total power acquired in the measurement of a conductor sphere. In this case, the distance of the blocks is 20 cm. The result was very similar when the distance is 10 cm or 15 cm.

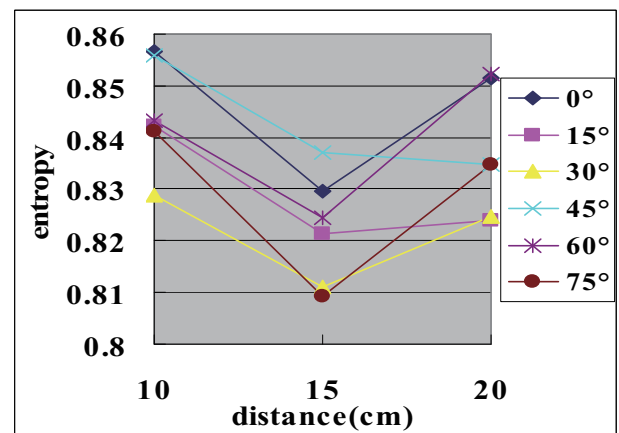


Figure 5. Relationship between entropy and the distance of the blocks.

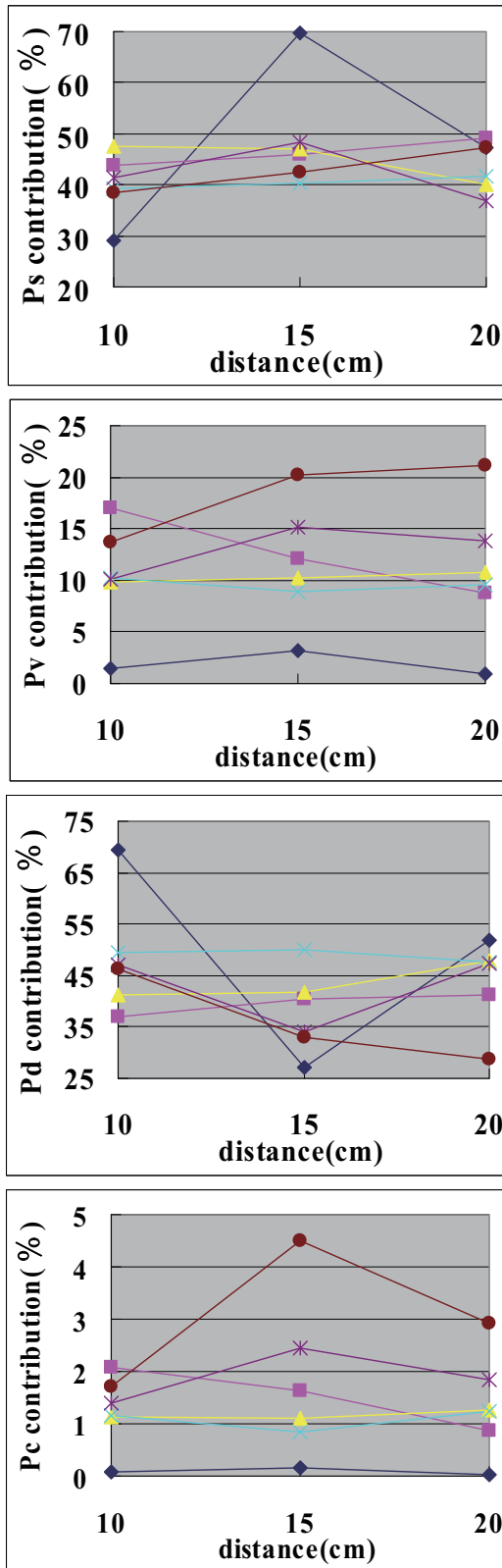


Figure 6. Relationship between four-components and the distance of the blocks. From upper to lower, surface scattering, volume scattering, double bounce scattering, and helix scattering are shown, respectively.

#### 4. APPLICATION TO L-BAND POLSAR FOR BUILDING CLASSIFICATION

In the experiment described in the previous section, two indices turned out to be available for the estimation of urban structural quantities; POA is for slant angle, and entropy is for density. In this section, to discriminate urban areas extracted from ALOS (Advanced Land Observing Satellite) / PALSAR (Phased Array type L-band Synthetic Aperture Radar) polarimetric images, a decision-tree classifier is proposed, which utilized the two indices.

##### 4.1 Data

Two regions on the Tokyo Bay coast were chosen for the target of the analysis. Observation date is July 17, 2006. Level 1.1 data of PALSAR onboard ALOS was analyzed. Level 1.1 is the range- and azimuth-compressed complex data (single look complex: SLC). It contains latitude-longitude information in a slant-range coordinate. Phase and amplitude of the scattered wave can be calculated from the image.

##### 4.2 Classification Algorithm

Figure 7 shows the classification algorithm using POA and entropy. Each step of the classification is explained below.

**4.2.1 Perpendicular Building Extraction using Four-Component Decomposition:** In the previous research (Iwasa *et al.*, 2009), it is ensured that the buildings perpendicular to the radar path are detectable using four-component decomposition. Based on this, pixels which have higher Ps and Pd value than certain thresholds are extracted as perpendicular building.

**4.2.2 Non-Building Area Removal using Total Power and Entropy:** Compared with building area, non-building areas (e.g. water, farmland, forest) generally have lower Total Power (*TP*), the summation of the elements of scattering matrix. Therefore, pixels which have lower *TP* value than certain threshold are extracted as non-building. Farmland perpendicular to the radar path, exceptionally, cannot be extracted utilizing *TP* thresholding, because it has as high *TP* value as building area. However, it is also found that such farmland has the lowest *H* value of all the land covering type. So, as a next step, pixels which have lower *H* value than certain threshold are extracted as perpendicular farmland, and they are added to non-building.

**4.2.3 Segmentation using POA:** Remaining pixels, which are regarded as slant buildings, are divided using  $\theta$  value into several categories. Before the segmentation,  $\theta$  value is averaged with  $7 \times 7$  filtering window. The segmentation is done so that each category approximately contains the same number of pixels.

**4.2.4 Segmentation using Entropy:** All building categories (including perpendicular buildings extracted at 4.2.1) are divided using *H* value into several clusters. Before the segmentation, *H* value is averaged with  $7 \times 7$  filtering window. The segmentation is done so that each cluster approximately contains the same number of pixels. After the segmentation, isolated pixels, whose all adjacent pixels are in other clusters, are reclassified.

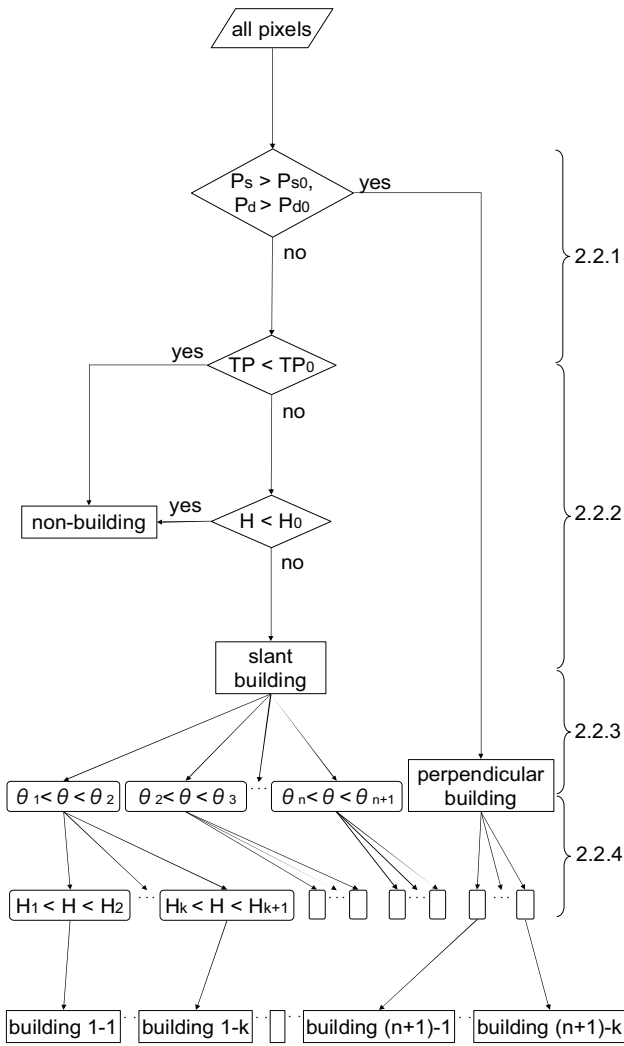


Figure 7. Building classification algorithm.

4.3 Results and Discussion

In the algorithm above, the number of the categories generated using POA value is set to 2, and the number of the clusters generated using entropy value is set to 6.

In Figure 8, classification result of Region 1 (around Odaiba) is compared with aerial photograph of the same region. From the classification result, it can be seen that the center part of the image is classified into low POA area, while the left part is into high POA area. Similar to this, aerial photograph shows that these two parts have different trend in slant angle of buildings. Moreover, perpendicular building area at the bottom left part of the classification result actually contains perpendicular buildings in aerial photograph. Consequently, segmentation of buildings according to their slant angle can be clearly done using both POA and four-component decomposition.

Figure 9 displays the comparison of classification result of Region 2 (around Kawasaki city) and aerial photograph of the same region. From the classification result, it can be seen that the upper side of the image is mainly classified into high POA area, while the lower side is mainly into low POA area. Correspondingly, it is found from aerial photograph that this

division roughly follows the distribution of the actual slant angle of the buildings. Extraction result of perpendicular buildings is also good. Furthermore, Figure 10 shows the details on the rectangle in Figure 9. In classification result, the left side and the right side of the green-colored part have different entropy value. Considering that there is a difference in density of the buildings between the left side and the right side of aerial photograph, entropy seems to be working well to detect the change of spatial distribution in this region.

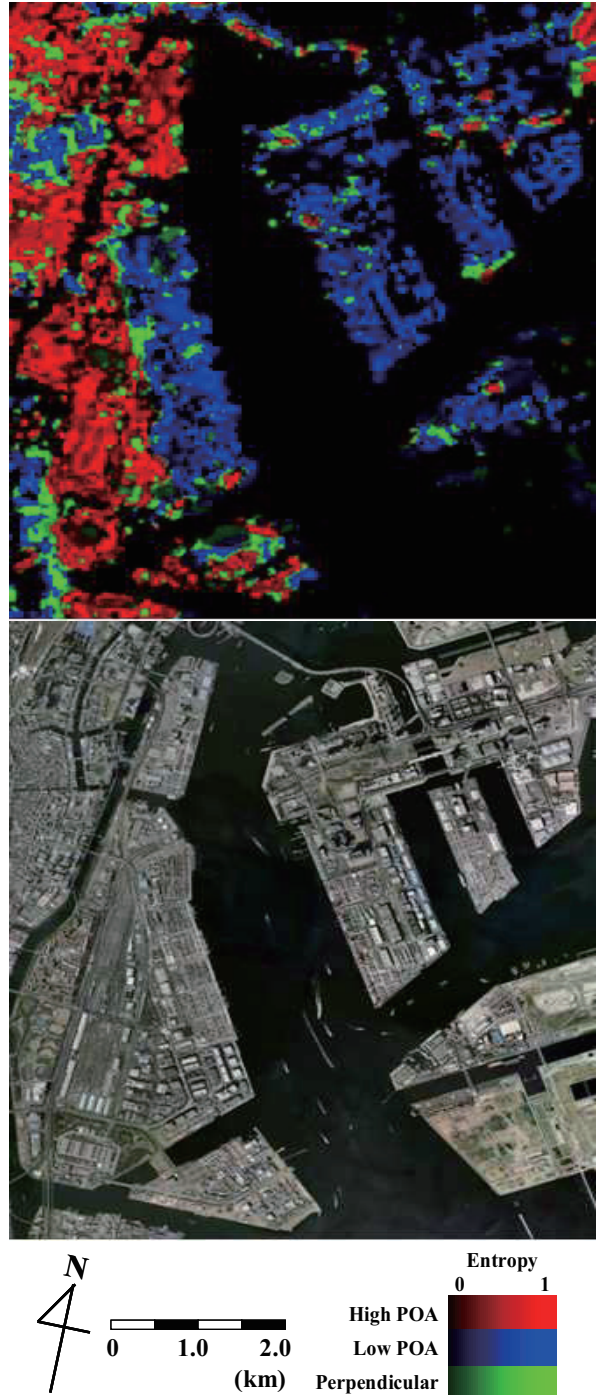


Figure 8. Classification result using the proposed decision-tree classifier in Region 1. (Upper) The classification result shows high POA area in red, low POA area in blue, and perpendicular building area in green. Tone of each color differs according to entropy value. (Lower) Aerial photograph from Google Earth.

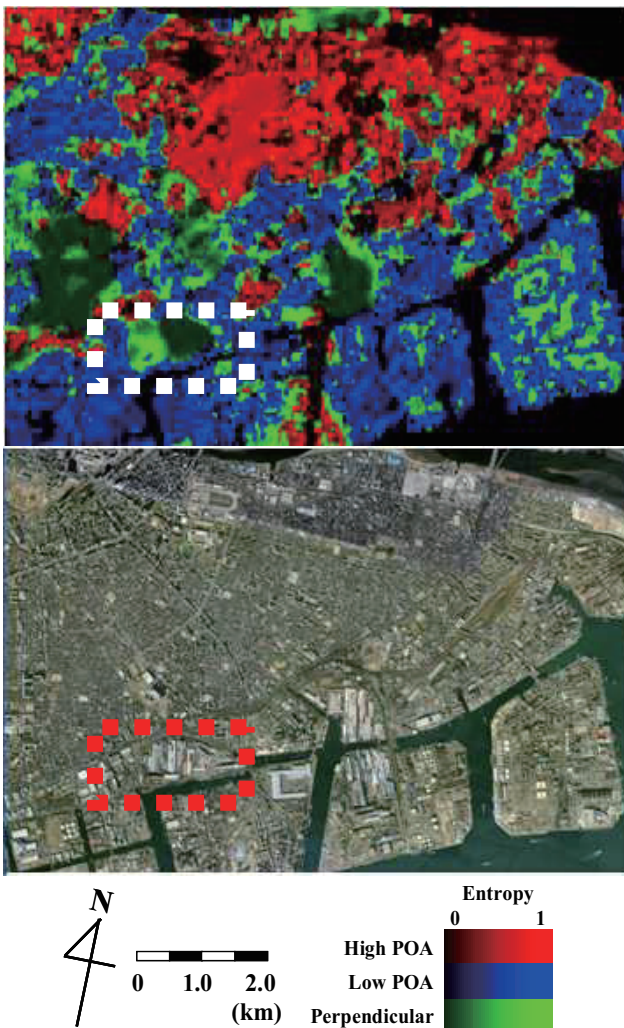


Figure 9. Classification result using the proposed decision-tree classifier in Region 2. (Upper) The classification result shows high POA area in red, low POA area in blue, and perpendicular building area in green. Tone of each color differs according to entropy value. (Lower) Aerial photograph from Google Earth.

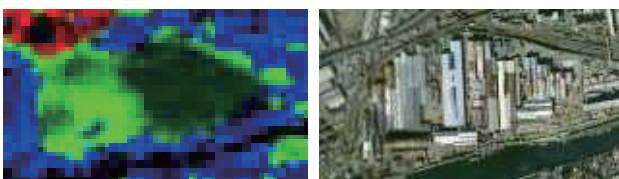


Figure 10. Zoom of the rectangle in Figure 9.

## 5. CONSLUTION

In this research, we examined the effectiveness of polarimetric indices as urban structural detectors through the analysis of laboratory experiment data, and we also applied some of the indices to ALOS/PALSAR data according to the decision-tree classifier based on the experimental results.

The experimental results demonstrated that POA has linear relationship with building slant angle. Also, it confirmed that entropy has the highest correlation with building density.

Through the analysis of satellite images, POA proved to classify buildings which are not perpendicular to the radar path according to their slant angle. In addition, we found that there are some areas where entropy distinguishes the difference of building density. Considering these result, the algorithm using polarimetric indices applied in this research seems effective for the classification of urban area extracted from POLSAR images.

One of the future works is detailed evaluation of the classification accuracy. We are going to calculate actual slant angle and density of the buildings from optical images as ground truth, and then compare them quantitatively with the classification results from POLSAR images. Moreover, we aim to develop the method which is usable independently of the topography of target areas. Therefore, effectiveness of used indices and algorithm should be tested not only in plain district like this research, but also in mountain district where POA and TP values are subject to ground slope.

## ACKNOWLEDGEMENTS

The authors would like to thank Y. Yamaguchi (Niigata University) and his students for offering experimental facilities and for many helpful comments. Further, the authors would like to thank the JAXA for providing the ALOS/PALSAR polarimetric data.

## REFERENCES

- Cloude, S. R., and E. Pottier, 1997. An entropy based classification scheme for land applications of polarimetric SAR, *IEEE Trans. Geosci. Remote Sens.*, 35, pp. 68–78.
- Dong, Y., B.C. Forser, and C. Ticehurst, 1998. A new decomposition of radar polarization signatures, *IEEE Trans. Remote Sens.*, 36(3), pp.933-939.
- Freeman, A., and S. L. Durden, 1998. A three-component scattering model for polarimetric SAR data, *IEEE Trans. Geosci. Remote Sens.*, 36(3), pp. 963-973.
- Iwasa, S., J. Susaki, and M. Tamura, 2009. Development of urban model using polarimetric synthetic aperture radar, *JSPRS Annual Conference*, pp.15-18, In Japanese.
- Kimura, H., K.P. Papathanassiou, and I. Hajnsek, 2005. Polarization orientation effects in urban areas on SAR data, *Proc. of the 2005 International Geosci. Remote Sens.*, pp.4863-4867.
- Uchida, N., K. Uchiyama, Y. Yamaguchi, and H. Yamada, 2009. A study on detection of urban area using Polarization Orientation Angle, *IEICE Technical Report*, 109(181), SANE2009-59, pp. 37-42, In Japanese.
- Yamaguchi, Y., T. Moriyama, M. Ishido, and H. Yamada, 2005. Four-component scattering model for polarimetric SAR image decomposition, *IEEE Trans. Geosci. Remote Sens.*, 43(8), pp. 1699-1706.
- Yamaguchi, Y., 2007. *Radar Polarimetry from Basics to Applications*, IEICE, pp.101-151.